




Imaging of Extrapinal Musculoskeletal Tuberculosis

Nuttaya Pattamapaspong 
and Wilfred C. G. Peh 

Contents

1	Introduction	326
2	Pathophysiology	326
3	Clinical Features and Complications	328
4	Imaging Features	329
4.1	Radiography	329
4.2	Computed Tomography	332
4.3	Magnetic Resonance Imaging	332
4.4	Ultrasound Imaging	335
4.5	Nuclear Medicine Imaging	336
5	Imaging Differential Diagnosis	346
5.1	Tuberculous Osteomyelitis	346
5.2	Tuberculous Arthritis	346
5.3	Tuberculous Soft Tissue Infection	347
6	Diagnosis Confirmation	348
7	Treatment	349
8	Conclusion	349
	References	349

N. Pattamapaspong (✉)
Department of Radiology, Faculty of Medicine,
Chiang Mai University, Chiang Mai, Thailand
e-mail: nuttaya.p@gmail.com; nuttaya.p@cmu.ac.th

W. C. G. Peh
Department of Diagnostic Radiology, Khoo Teck
Puat Hospital, Singapore, Republic of Singapore
e-mail: Wilfred.peh@gmail.com;
Wilfred.peh@ktph.com.sg

Abstract

Tuberculosis can lead to serious destruction of musculoskeletal structures such as the bones, joints, and soft tissues. Early diagnosis of musculoskeletal tuberculosis is important in order to minimize structural damage and prevent permanent complications. The diagnosis requires a high degree of awareness as the clinical presentation may be indolent, non-specific, and may mimic other disease processes. Tissue destruction from tuberculous granulomas produces some characteristic patterns which can be demonstrated by imaging studies. Radiography, ultrasound imaging, computed tomography, and magnetic resonance imaging help in detection of the disease, guide appropriate laboratory investigation and surgical management, as well as in the evaluation of treatment outcome. Whole-body [Fluorine-18]-fluoro-2-deoxy-D-glucose positron-emission tomography has a gradually increasing role in the detection of multifocal lesions and disease monitoring. Knowing the characteristic imaging features and potential mimics aids in timely diagnosis and treatment of musculoskeletal tuberculosis.

Abbreviations

CT	Computed tomography
MRI	Magnetic resonance imaging
TB	Tuberculosis

1 Introduction

Musculoskeletal tuberculosis (TB) is an important cause of mortality and morbidity worldwide. Cases are rising because of the steadily increasing number of immunocompromised hosts such as patients with human immunodeficiency virus (HIV) infection, immunosuppressive treatment, advanced age, and also a rise in immigration from countries with a high disease prevalence (Arora and Chopra 2019; Suarez et al. 2019; World Health Organization 2021). Appendicular involvement, although less common than spinal TB, can lead to serious bone and joint destruction. The indolent and diverse clinical presentation often mimics many other diseases, and may cause a delay in diagnosis. The emergence of multidrug-resistant strains increases the difficulty in treatment and control of disease spread. Early imaging diagnosis plays an important role in directing appropriate laboratory investigation, hence allowing timely diagnosis and treatment.

2 Pathophysiology

TB affects the musculoskeletal system, causing osteomyelitis, arthritis, or soft tissue infection. The organism reaches the musculoskeletal system via hematogenous spread or by direct inoculation. Hematogenous spread is more common and will be discussed in more detail in the following paragraphs. The disease either presents during the primary spread of the organism or as a reactivation, usually when host immunity decreases. At the site of infection, the TB bacilli induce a granulomatous inflammatory reaction that consists of epithelioid cells, lymphocytes, and multinucleated giant cells, forming either

caseating or noncaseating granulomas (Natarajan et al. 2020). The host inflammatory response results in liquefactive and caseous necrosis, tissue destruction, and abscess formation. The infective focus then spreads to the surrounding structures. In the late stage of the disease, the granulomatous lesions may calcify (Sharma et al. 1978).

The metaphysis of long bones and large weight-bearing joints, such as the hip and knee, are commonly affected because of their rich vascular supply (Pigrau-Serrallach and Rodríguez-Pardo 2013; Natarajan et al. 2020). The predilection for the location of osteomyelitis depends on the distribution of intraosseous vascular structures according to age. In infants younger than 1.5 years of age, transphyseal spread is common, due to vessels crossing the growth plate. In children aged between one and 16 years, the metaphysis is the most common site, as the epiphyseal growth plate acts as a natural barrier to the spread of infection. However, isolated epiphyseal lesions may still occur, owing to the presence of the nutrient artery of the epiphysis. In adults, vascular distribution in form of communicating metaphyseal and epiphyseal vessels allows the infection to reach subchondral bone (Wang et al. 1999; Resnick 2002a; Ranson 2009) (Fig. 1).

Tuberculous arthritis may result from primary spread via subsynovial vessels, or be secondary to osteomyelitis or infected para-articular tissue (De Backer et al. 2006) (Fig. 2). As the exudative fluid in tuberculous arthritis lacks proteolytic enzymes, the cartilage is usually spared until later stages of the disease (Akeson et al. 2002). The pattern of cartilage destruction reflects the growth of granulation tissue which can be along the free surface of cartilage, between the cartilage and subchondral bone, or result from penetration through the cartilage (Resnick 2002b) (Fig. 2).

Soft tissue infections, including pyomyositis, bursitis, tenosynovitis, and subcutaneous tissue abscesses, can present as a primary affected site but is more commonly a complication of

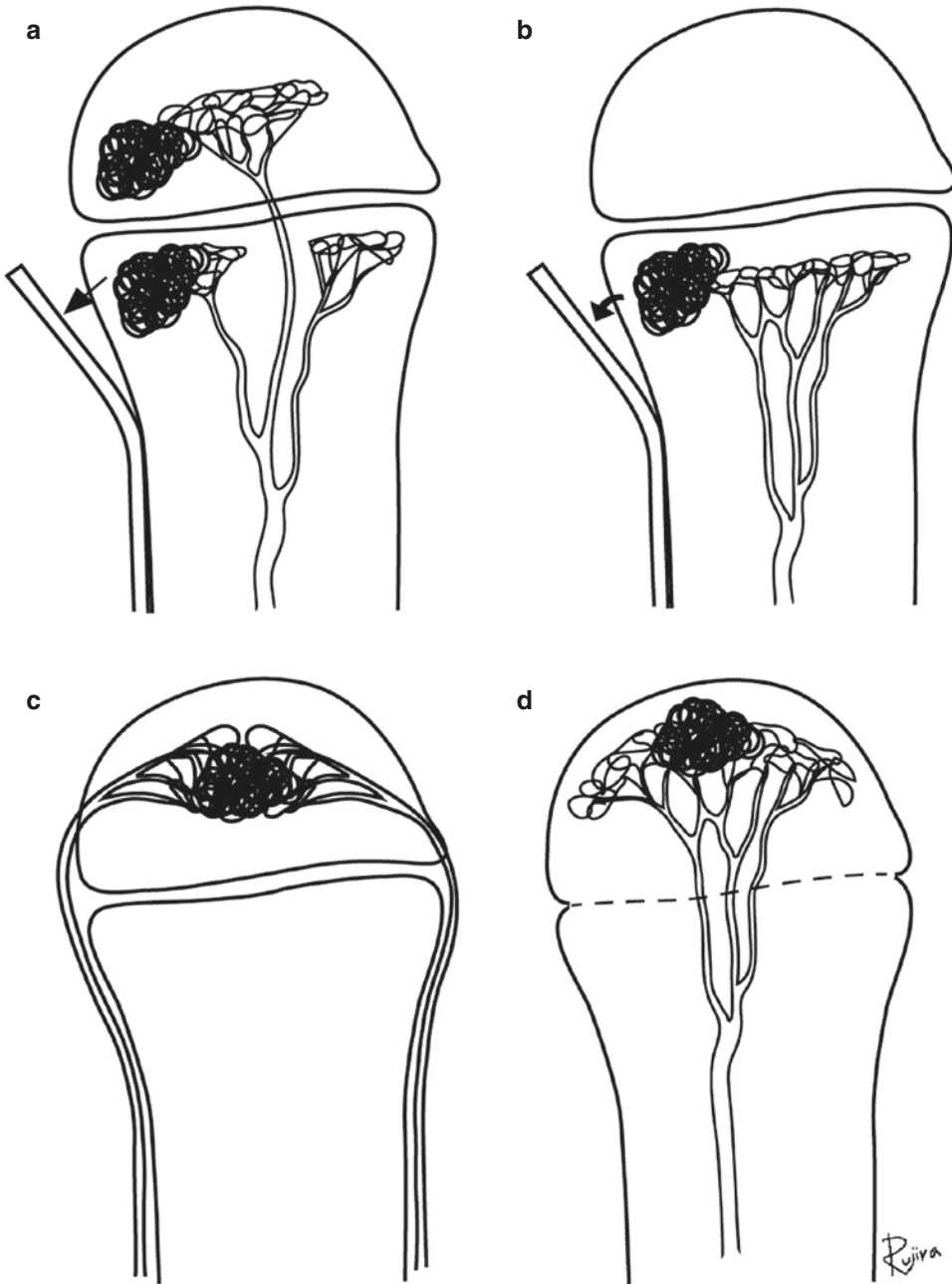


Fig. 1 Location of osteomyelitis and distribution of intraosseous vascular structures according to age. (a) In infants aged less than 1.5 years, infection in the metaphysis spreads via vessels traversing the growth plate leading to infection of the epiphysis. (b) In children aged 1–16 years, infection has predilection for the metaphysis because of its rich vascular supply. The growth plate acts as a natural barrier to infection spreading to the epiphysis.

The infection in the metaphysis may spread under the periosteum and extend to the surrounding soft tissues (arrows in a and b). (c) Isolated epiphyseal osteomyelitis may occur due to spread via the epiphyseal nutrient artery. (d) In adults, epiphyseal vessels passing through the closed physis allow infection to reach subchondral bone. Osteomyelitis in the epiphysis and subchondral bone can spread to the joint resulting in tuberculous arthritis

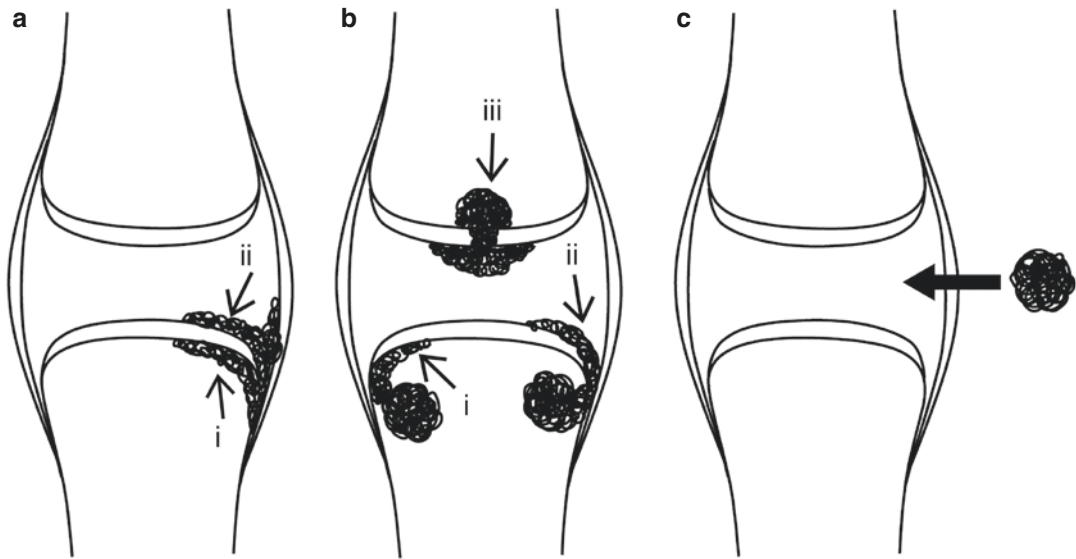


Fig. 2 Patterns of spread causing tuberculous arthritis and cartilage destruction. Joint infection spreads from (a) subsynovial vessels, (b) osteomyelitis, or (c) infected para-articular soft tissues. Destruction of the cartilage by

granulation tissue can be (i) deep from subchondral bone, (ii) over the cartilage surface, or (iii) through penetration of the cartilage

osteomyelitis or arthritis. Tuberculous tenosynovitis and bursitis initially develop as a serous effusion, followed by synovial thickening, and accumulation of tissue debris and caseous material. Eventually, debris and synovial thickening become prominent and there is minimal effusion. Tenosynovitis may lead to tendon tethering or rupture (Jaovisidha et al. 1996).

3 Clinical Features and Complications

Musculoskeletal TB is a disease that affects all age groups but there is a predilection for children and the elderly (Perez-Velez and Marais 2012; Arora and Chopra 2019). Clinical features of musculoskeletal TB are variable and non-specific. Infected patients can present with chronic pain, limb deformity, dislocation, pathological fracture, palpable mass as a result of abscess formation, or draining skin sinus. Fever is infrequent and is mostly associated with disseminated infection (Naidoo et al. 2017). Multifocal lesions

occur in 7–11% of patients and are commonly associated with HIV infection, children, or poor physical status (Prasad et al. 2012; Pigrau-Serrallach and Rodríguez-Pardo 2013; Naidoo et al. 2017; Suarez et al. 2019). Not all lesions are symptomatic, and different stages of destruction and healing can be expected as a result of multiple episodes of hematogenous seeding of the organism and variable local tissue immunity.

The major predisposing factors of musculoskeletal TB are conditions leading to immunosuppression, caused by diseases or treatment (Hodkinson et al. 2009; Lin et al. 2009). Tissue injury, either by trauma or surgery, is a predisposing factor because of increased vascular supply and impairment of the local immune system. Tuberculous infection has been reported following different types of surgery such as fracture fixation (Kumar et al. 2006), reconstruction of the anterior cruciate ligament of the knee (Nag et al. 2009), and sternotomy (Gopal et al. 2007). Inflammatory joint disease may also predispose to tuberculous arthritis (Bryan et al. 1982; Hortas et al. 1988). Prosthetic joint infection due to TB

is uncommon. Three pathogenic mechanisms have been reported: (1) Active tuberculous arthritis present at the time of surgery but not known to clinician; (2) Hematogenous spread from a distant focus; and (3) Surgical trauma resulting in activation of previous unknown TB (Hugate and Pellegrini 2002; Khater et al. 2007; Carrega et al. 2013; Harwin et al. 2013).

Bone and joint infections often subsequently progress to soft tissue abscesses. Tuberculous abscess typically has a minimal inflammatory response, and is also called a cold abscess. If untreated, the soft tissue abscess may form a sinus tract which drains to the skin. In the immature skeleton, bone and joint tuberculosis may cause limb length discrepancy and deformity. In tenosynovitis of the wrist, thickened synovial tissue and debris can envelop the median nerve, resulting in the carpal tunnel syndrome (Hassanpour and Gousheh 2006).

4 Imaging Features

4.1 Radiography

Radiographs are the main modality used in the detection of musculoskeletal infection. Due to the typically late and indolent clinical presentation, radiographs commonly reveal the advanced stages of disease with considerable structural destruction. The features of tuberculous osteomyelitis are a well-defined osteolytic lesion usually located in the metaphysis of long bones with or without sclerotic reaction, cortical expansile remodeling, sequestrum, and periostitis. Transphyseal spread is a characteristic feature of tuberculous osteomyelitis, a finding which is unusual for bacterial infection (De Vuyst et al. 2003) (Figs. 3, 4, and 5). An isolated epiphyseal lesion resulting from epiphyseal vessel spread may sometimes occur (Fig. 6)

Multifocal tuberculous osteomyelitis, also called osteitis cystica tuberculosa multiplex, is an unusual form of osteomyelitis that occurs in children more often than in adults (Shikhare et al.



Fig. 3 Tuberculous osteomyelitis with transphyseal spread in an 8-month-old male infant who had swelling of the leg for 1 month. Frontal radiograph shows an osteolytic lesion in the metaphysis with bone expansion and thick laminated periosteal reaction. Note the osteolytic lesion in the epiphysis (arrow) indicating transphyseal spread



Fig. 4 Tuberculous osteomyelitis of the calcaneus in a 10-year-old girl who presented with a draining sinus in the heel. Lateral radiograph shows an osteolytic lesion with sclerotic reaction. Note the cortical bone destruction corresponding to the location of the sinus (arrows)

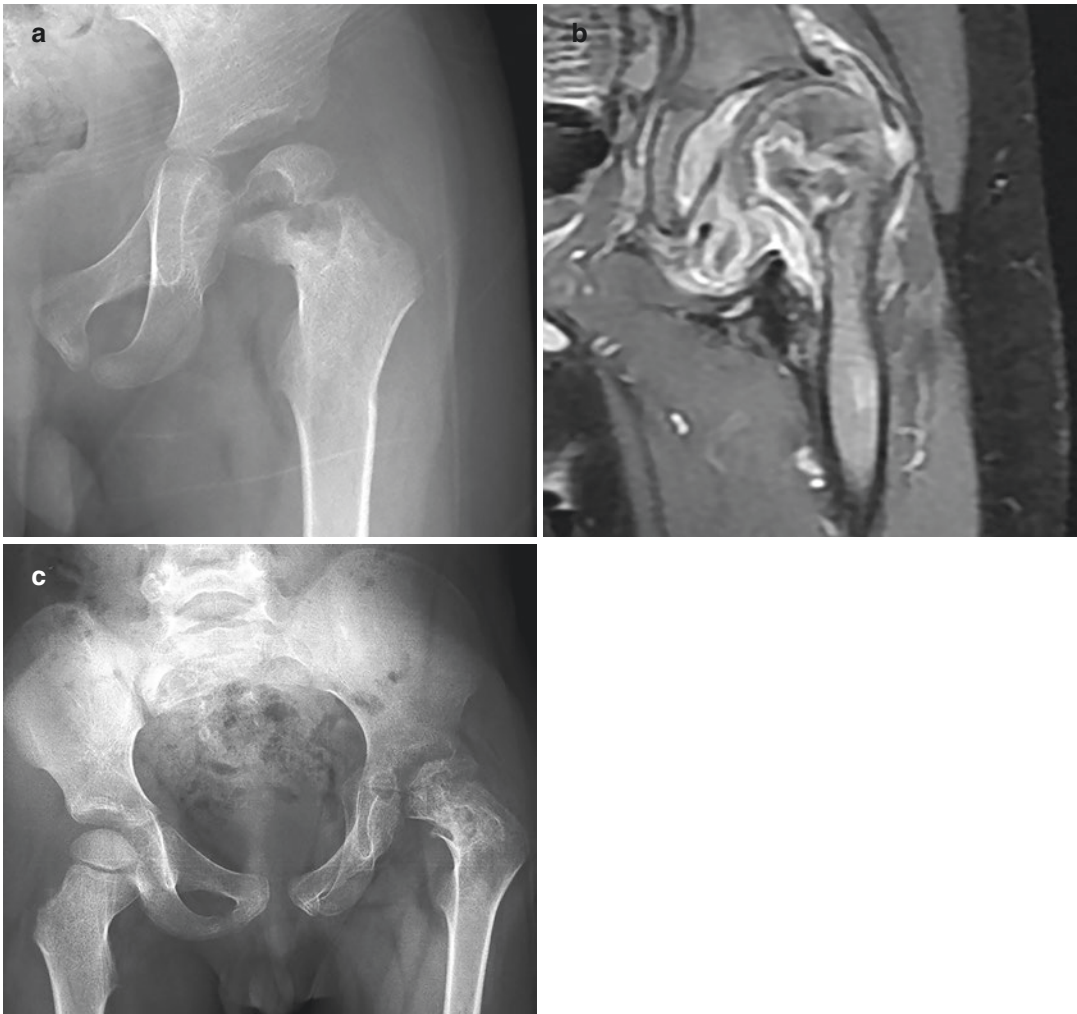


Fig. 5 Tuberculous osteomyelitis with transphyseal spread and arthritis in a 4-year-old girl. (a) Frontal radiograph shows an osteolytic lesion in the metaphysis with extension to the proximal femoral epiphysis. (b) Coronal contrast-enhanced fat-suppressed T1-weighted MR image shows transphyseal extension of the intraosseous abscess and synovial enhancement indicating joint involvement.

(c) Frontal radiograph taken at 2-year follow-up after treatment shows a flattened left femoral epiphysis mimicking the changes of Perthes disease. Note the sclerotic changes due to healed osteomyelitis. (Courtesy of Dr. Thanat Kanthawang, Faculty of Medicine, Chiang Mai University, Thailand)

2011). The disease manifests radiographically as well-defined osteolytic lesions resembling bone cysts of variable sizes. Sclerotic changes at the lesion margins are usually minimal and when present support evidence of healing (Tiwari et al. 2007) (Fig. 7).

Tuberculous dactylitis or osteomyelitis of the short tubular bone of hands and feet commonly occurs in younger patients, particularly children aged less than 6 years (Ranjan et al. 2019). These patients often present with soft tissue swelling and flexion deformity. Characteristic



Fig. 6 Tuberculous epiphyseal osteomyelitis in a 2-year-old boy who had right knee swelling for 4 months. Frontal radiograph of the knee shows an osteolytic lesion in the femoral epiphysis

radiographic features include an osteolytic lesion, fusiform expansion of the bone and thick periosteal reaction, leading to the term spina (short bone) ventosa (inflated with air) (Fig. 8). In the mild form of the disease, dactylitis causes soft tissue swelling and periosteal reaction.

The radiographic hallmark of tuberculous arthritis, described as the Pheinstier triad, consists of marginal bone erosions, juxta-articular osteoporosis, and relatively preserved joint space (Pheinstier and Hatcher 1933) (Figs. 9, 10, and 11). Large subchondral bone destruction, due to intraosseous abscesses, may be present (Fig. 10). Widespread disease may also occur in the interconnecting joints of the wrist and midfoot (Dhillon and Nagi 2002; Hsu et al. 2004) (Fig. 11). Soft tissue abscesses, tenosynovitis, or bursitis can lead to a large soft tissue mass detectable on radiographs (Fig. 10a). Associated soft tissue calcification is a suggestive sign of tuberculous infection (Sharma et al. 1978) (Fig. 12).

Apart from structural damage by granulomatous formation, radiographs can demonstrate

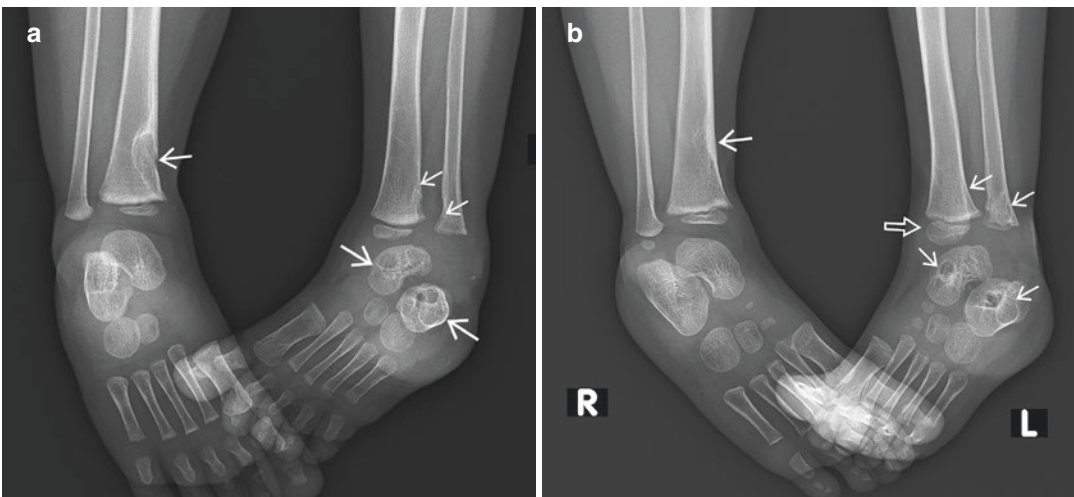


Fig. 7 Multifocal tuberculous osteomyelitis in a 16-month-old boy. (a) Frontal radiograph of both ankles shows multifocal osteolytic lesions (arrows). (b) 8-month follow-up frontal radiograph shows variable degrees of

sclerotic change around the lesions indicating different stages of healing. Note overgrowth of the medial left tibial epiphysis (open arrow)



Fig. 8 Tuberculous dactylitis (or spina ventosa). Frontal radiograph of the ring finger shows an ill-defined osteolytic lesion of the proximal phalanx with cortical destruction. There is surrounding soft tissue swelling. (Courtesy of Prof. Mohamed Fethi Ladeb, MT Kassab Institute of Orthopaedics, Tunis, Tunisia)

complications such as pathological fracture (Fig. 13), dislocation (Figs. 14 and 15), limb length discrepancy, and deformities. Enlarged epiphyses result from reactive hyperemia affecting the growing ossification center (Fig. 7b). In the hip, gradual joint destruction in the weight-bearing joint causes bone remodeling and acetabular protrusion (Fig. 16a). Fibrous ankylosis occurs as an end-stage of the disease (De Vuyst

et al. 2003). Bony ankylosis is uncommon in tuberculosis except in cases with surgical intervention (Parsa et al. 2018).

4.2 Computed Tomography

Computed tomography (CT) helps better demonstrate the features of TB detected by radiographs, particularly bone erosions, sequestrum (Fig. 10b–d), pyomyositis, and soft tissue calcification (Figs. 15b, c and 17). CT enables detailed evaluation of abscess extension, internal organ involvement, and disseminated disease (Fig. 18). CT is particularly useful in the assessment of chest wall infection, which has a predilection for the sternal margin because of spread of infection via the internal mammary lymph nodes (Bergeron et al. 2017) (Fig. 19a). Other affected sites are the sternoclavicular joint, costochondral junction, rib shafts, and costovertebral joints (Morris et al. 2004). Mediastinal extension is well demonstrated by CT (Fig. 20). CT is also useful for guiding biopsy.

4.3 Magnetic Resonance Imaging

Magnetic resonance imaging (MRI) is the most useful modality for the evaluation of musculoskeletal TB, as it provides a good demonstration of inflammatory processes in bones, joints, and soft tissues (Figs. 5b, 9b–d, and 19b, c). The minimal inflammatory response of the tissues around an abscess is a characteristic finding of tuberculous infection (Fig. 21). Sinus formation is seen as “tram-track” enhancement extending from the infected site to the skin (Figs. 14c, d and 22). In children, MRI allows better evaluation of transphyseal spread, articular involvement, and infection of the unossified part of the epiphysis (Figs. 5b and 23).

A characteristic sign of abscess formation on MRI is the presence of a penumbra, which refers to the T1-hyperintense wall of abscess

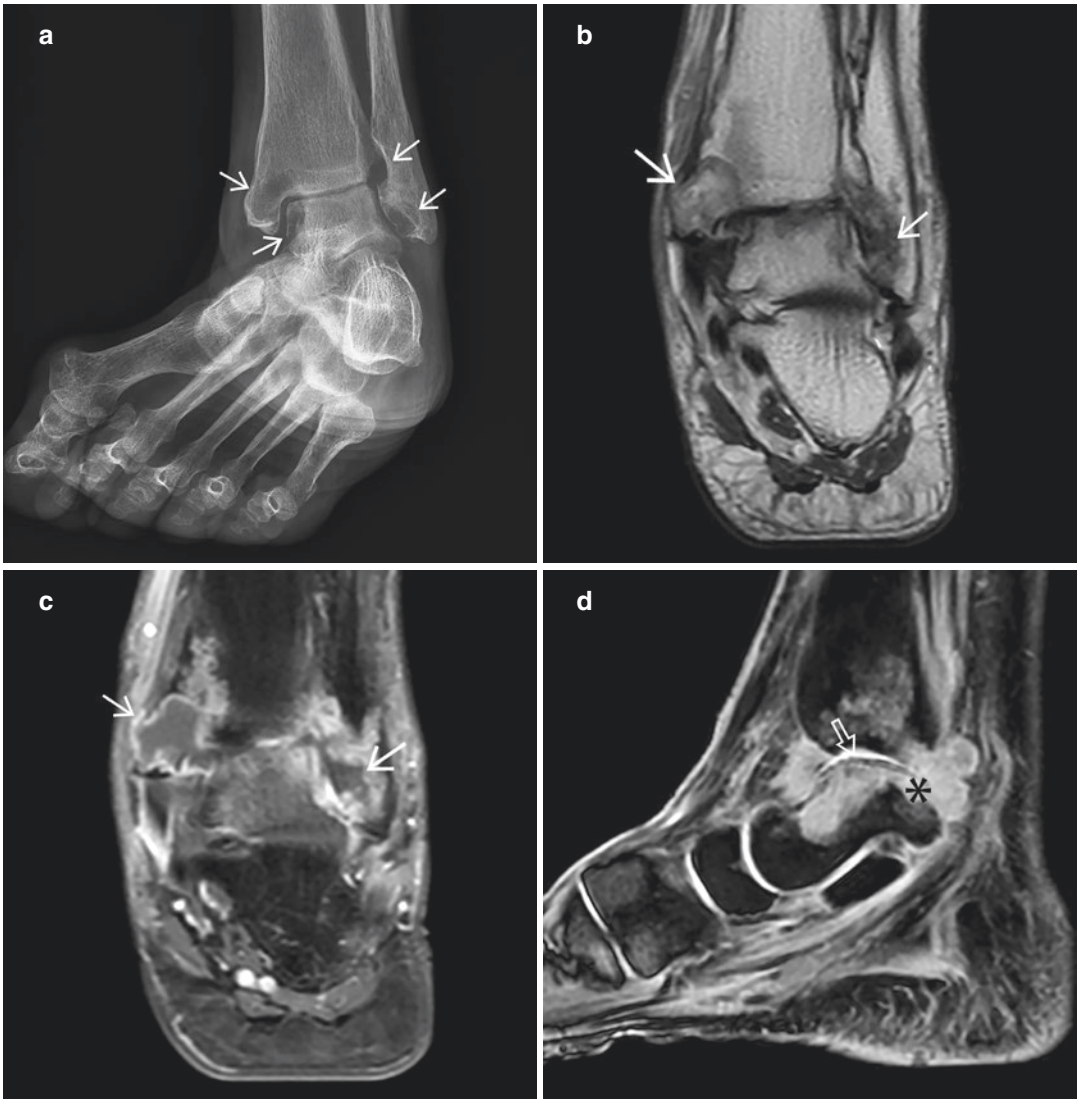


Fig. 9 Tuberculous arthritis in a 68-year-old woman who had chronic left ankle pain. **(a)** Frontal radiograph shows erosions (arrows) with relatively spared joint spaces. Coronal **(b)** T2-weighted and **(c)** contrast-enhanced fat-suppressed T1-weighted MR images show large bone ero-

sions with enhanced granulation tissue (arrows). **(d)** Sagittal MR image using the water-selective cartilage (WATSc) sequence shows a relatively intact cartilage surface (open arrow) with subchondral extension of the granulation tissue (*)

representing vascularized granulation tissue (Grey et al. 1998) (Fig. 23). This penumbra sign has a high specificity (96%) for chronic abscesses and helps in differentiating musculoskeletal infection from tumors (McGuinness et al. 2007). However, the sign is not specific to TB, and

abscess formation from other organisms can also produce this sign. Rarely, this sign has also been reported in chondrosarcoma, eosinophilic granuloma, fibrous dysplasia, pigmented villonodular synovitis, and benign cystic lesions (Grey et al. 1998; McGuinness et al. 2007).

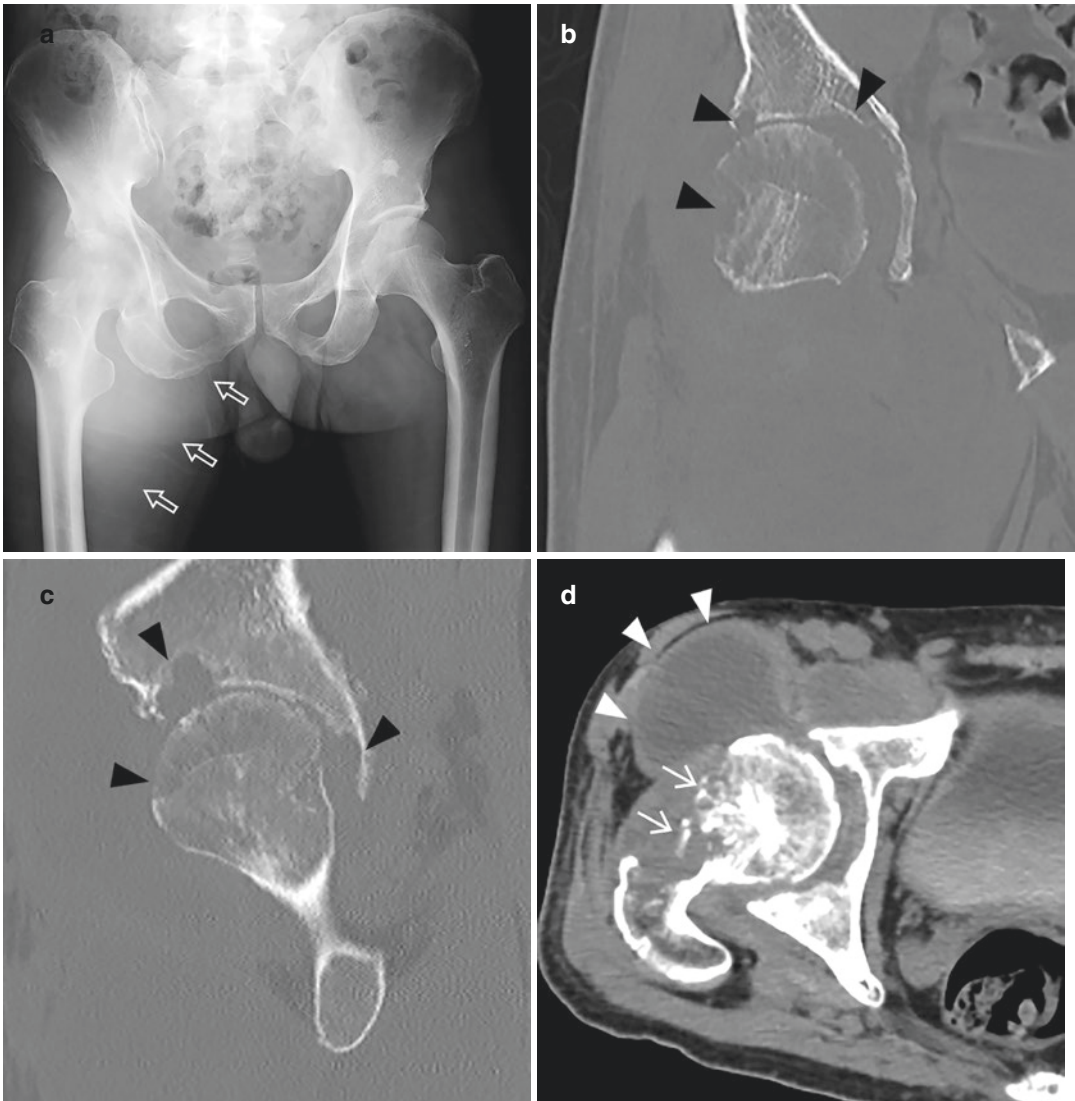


Fig. 10 Tuberculous arthritis in a 54-year-old man who had right hip pain and a groin mass for 4 months. **(a)** Frontal radiograph shows right hip joint destruction and juxta-articular osteoporosis. Note the large soft tissue shadow in the right upper thigh (open arrows). **(b)** Coronal

and **(c)** sagittal CT images show large bone erosions around the right hip joint (black arrowheads). **(d)** Axial contrast-enhanced CT image shows sequestra (arrows) and a large para-articular abscess (arrowheads)

In tuberculous arthritis, MRI can demonstrate the cartilage and bone destruction caused by granulation tissue. With the lack of proteolytic enzymes, focal areas of relatively intact cartilage may be present between the areas of granulation tissue (Fig. 9d). Synovial proliferation with heterogeneous intermediate to hypoin-

tense signal on T2-weighted images is found in approximately 40% of tuberculous arthritis (Sawhani et al. 2003) (Fig. 16b). Tissue components in caseous necrosis, including fibrosis, macrophage infiltration, and free radicals from macrophage by-products, contribute to T2-hypointense signal in tuberculous synovitis



Fig. 11 Tuberculous arthritis in a 33-year-old man who had a right wrist pain for 3 weeks. Frontal radiograph shows extensive bone erosions in the interconnecting joints of the wrist, and prominent juxta-articular osteoporosis with relatively preserved joint spaces

(Suh et al. 1996; Sawlani et al. 2003) (Fig. 16b). Presence of rice bodies in the joint, bursa, or tendon sheath is a sign of chronic synovitis, a feature also sometimes seen in tuberculous infection. Rice bodies have been described in various rheumatic diseases including rheumatoid arthritis, juvenile idiopathic arthritis, or osteoarthritis (Griffith et al. 1996; Forse et al. 2012; Subramaniam et al. 2012). Rice bodies represent debris whose shape resembles grains of rice, and consists of fibrin collagen and mononuclear cells (Popert 1985) (Fig. 24).

4.4 Ultrasound Imaging

Ultrasound (US) imaging is a good modality for the detection of joint effusion, synovial thickening, bone erosion, and soft tissue extension. There is often very marked synovial thickening which contrasts with low volume joint effusion. Para-articular

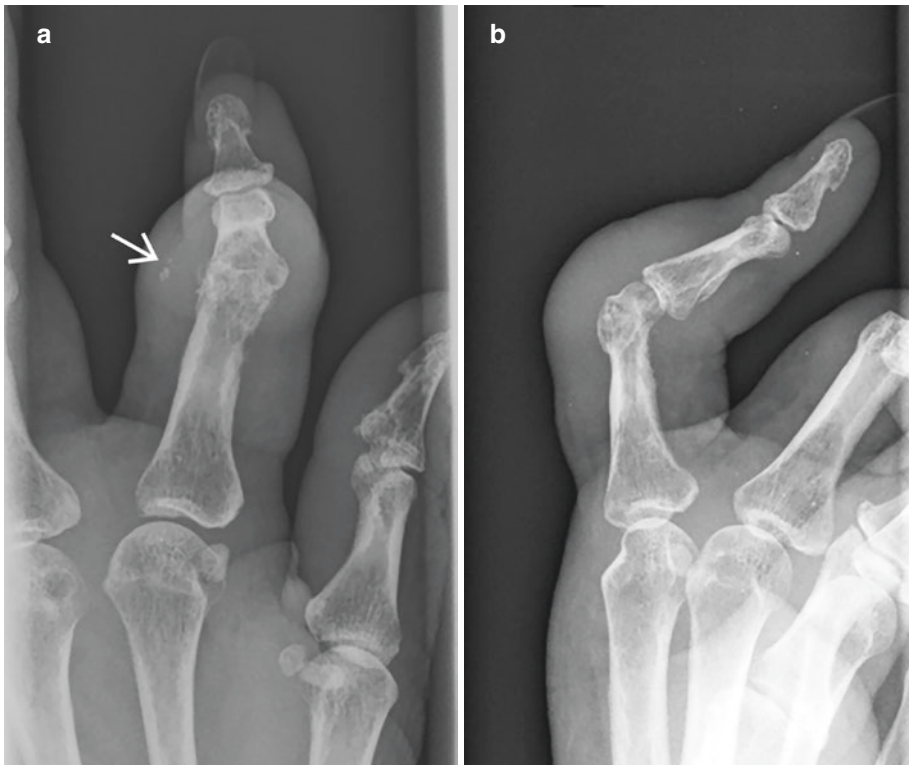


Fig. 12 Soft tissue tuberculosis with calcification in a 57-year-old woman who had index finger swelling for 1 month. (a) Frontal and (b) lateral radiographs show soft tissue swelling, flexion deformity, subluxation of the

proximal interphalangeal joint, and small soft tissue calcifications (arrow). Surgery revealed soft tissue abscess, and rupture of the extensor digitorum tendon and joint capsule



Fig. 13 Tuberculous osteomyelitis with pathological fracture in a 91-year-old woman. Frontal radiograph shows an oblique fracture through a permeative osteolytic lesion in the proximal phalanx of the finger

abscess, rice bodies, and granulomatous calcifications are well detected (Fig. 25). US imaging can also be used for guiding fluid aspiration.

4.5 Nuclear Medicine Imaging

Nuclear medicine imaging studies allow detection of multifocal infection and monitoring of disease but its utility limited by low specificity. Three-phase ^{99m}Tc methylene diphosphonate (MDP) bone scintigraphy is positive in active and healing osteomyelitis. Gallium scintigraphy and labeled leukocyte imaging help identification of active infection (Palestro et al. 2006). Whole-body [Fluorine-18]-fluoro-2-deoxy-D-glucose positron-emission tomography (^{18}F -FDG PET) has a gradually increasing role in detecting multifocal lesions, assessing disease activity, and monitoring response to treatment (Ankrah et al. 2016). Active TB has avid tracer uptake (Fig. 26). Since ^{18}F -FDG is a non-specific tracer, it may cause a false-positive diagnosis in patients being evaluated for tumor metastasis.



Fig. 14 Tuberculous arthritis with joint subluxation in a 49-year-old woman with connective tissue disease who had left wrist pain and draining sinus. (a) Frontal radiograph shows extensive destruction of the carpal and adjacent bones of the wrist with juxta-articular osteoporosis.

(b) Lateral radiograph shows dorsal subluxation of the distal radioulnar joint (arrow). Axial (c) short tau inversion recovery (STIR) and (d) contrast-enhanced fat-suppressed T1-weighted MR images show a "tram-track" sinus tract (arrowheads)

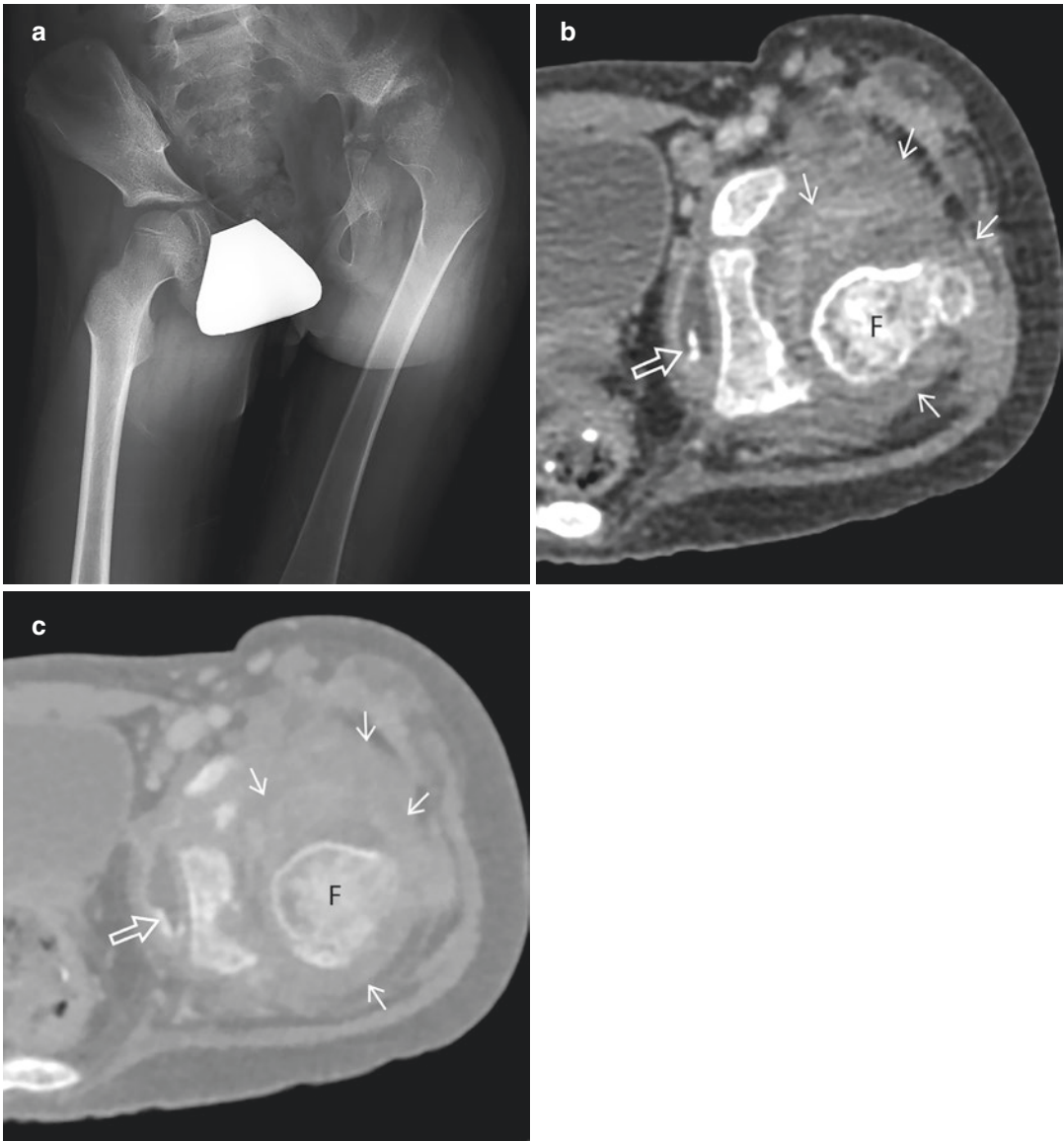


Fig. 15 Tuberculous arthritis with subluxation in a 6-year-old girl who had left hip pain and limb length discrepancy. (a) Frontal radiograph shows destruction of the left hip joint and shortening of the left limb. Axial CT

images obtained in (b) soft tissue and (c) bone window settings show distension of the joint by a large effusion (arrows), posterior subluxation of the femoral head (F), and a calcified abscess (open arrow)

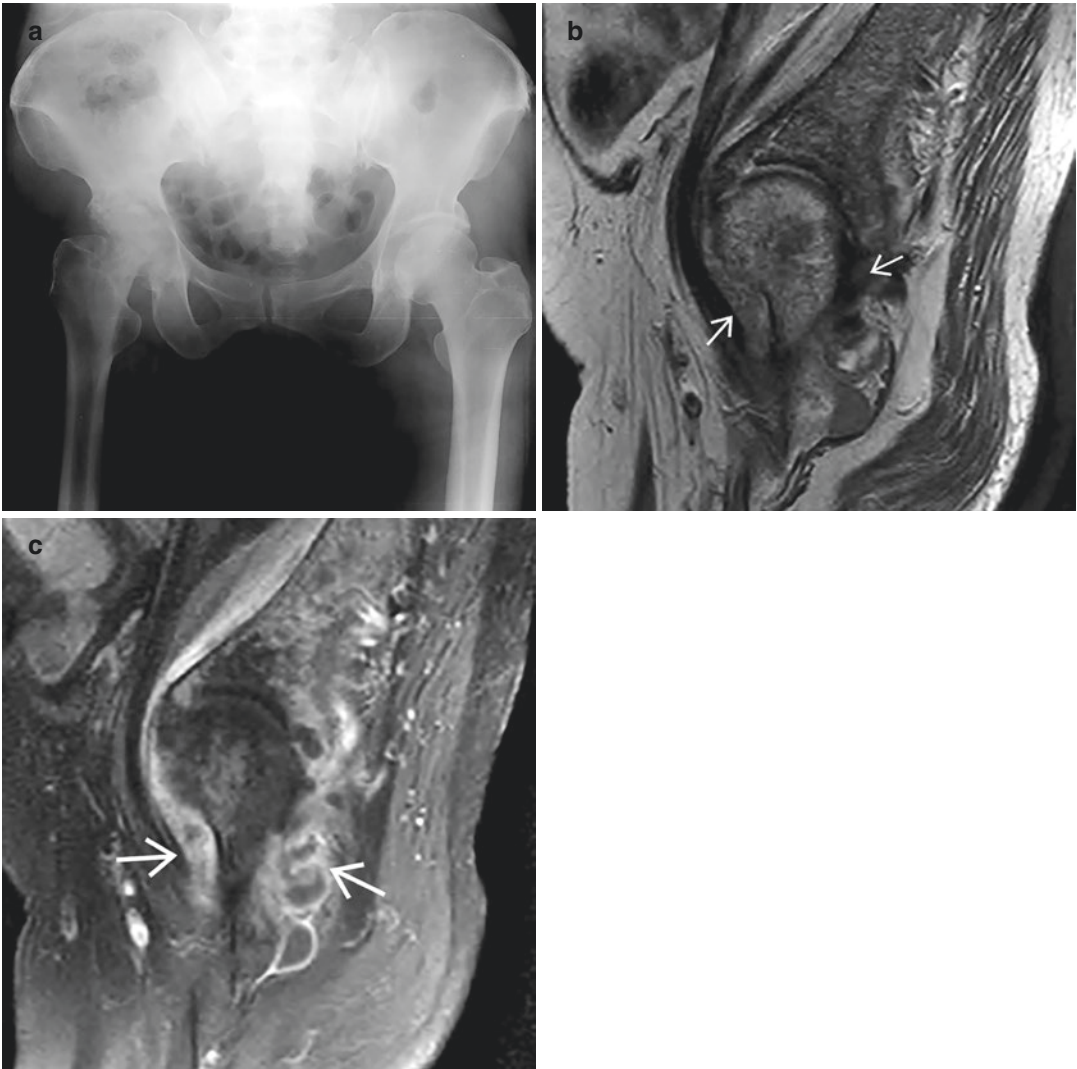


Fig. 16 Tuberculous arthritis in a 74-year-old woman who had a right hip pain for 2 weeks. (a) Frontal radiograph shows destruction of the right hip joint with medial wall deformity of the acetabulum (protrusio acetabuli).

Sagittal (b) T2-weighted and (c) contrast-enhanced fat-suppressed T1-weighted MR images show T2-hypointense synovitis with rim enhancement (arrows)

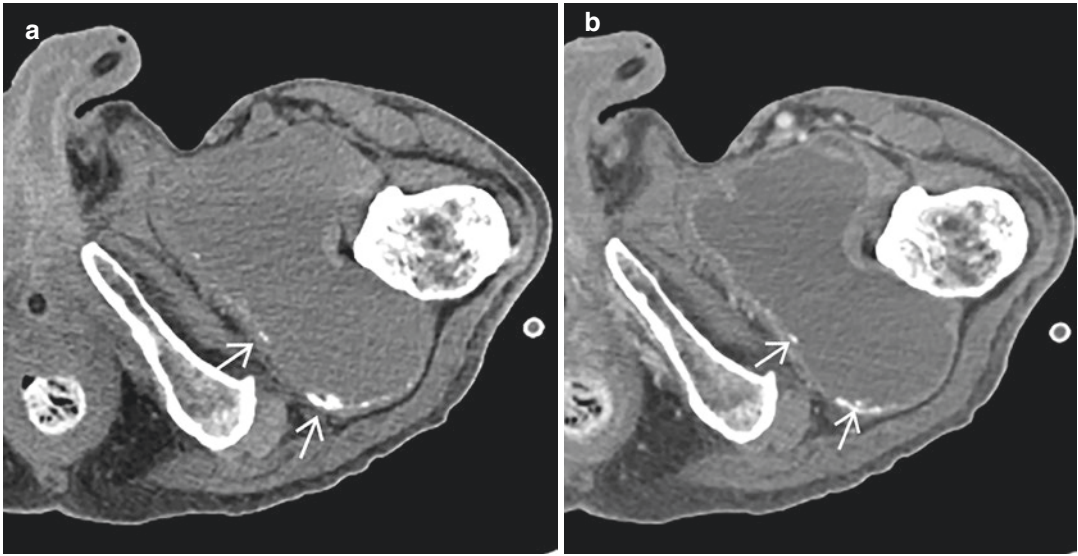
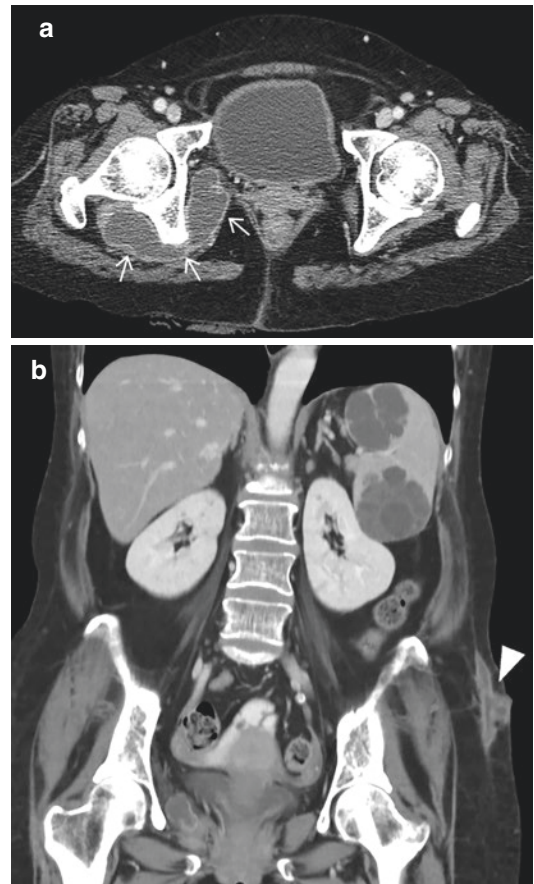


Fig. 17 Tuberculous soft tissue abscess in a 65-year-old man who had a slow-growing mass in the left thigh for 1 year. Axial (a) unenhanced and (b) contrast-enhanced CT

images show a large abscess with rim-enhancing wall and calcifications (arrows)

Fig. 18 Disseminated tuberculosis in a 50-year-old woman with connective tissue disease. (a) Axial contrast-enhanced CT image shows a deep soft tissue abscess adjacent to the right posterior hip joint and posterior ischium with extension deep to the gluteus minimus and obturator internus muscles (arrows), lateral to the ischiorectal fossa. (b) Coronal contrast-enhanced CT image shows splenic abscesses and a subcutaneous tissue abscess with a sinus tract in the left buttock (arrowhead)



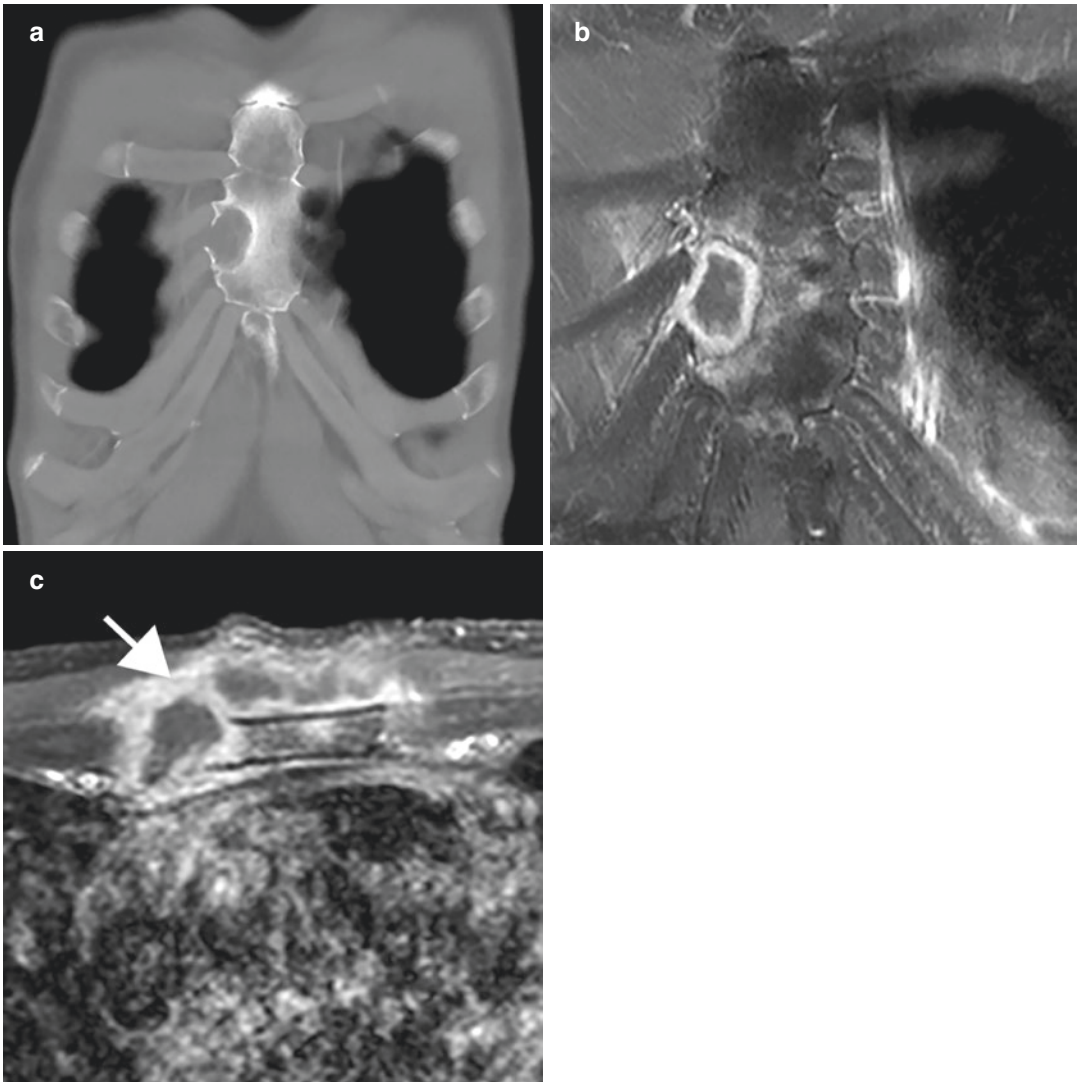


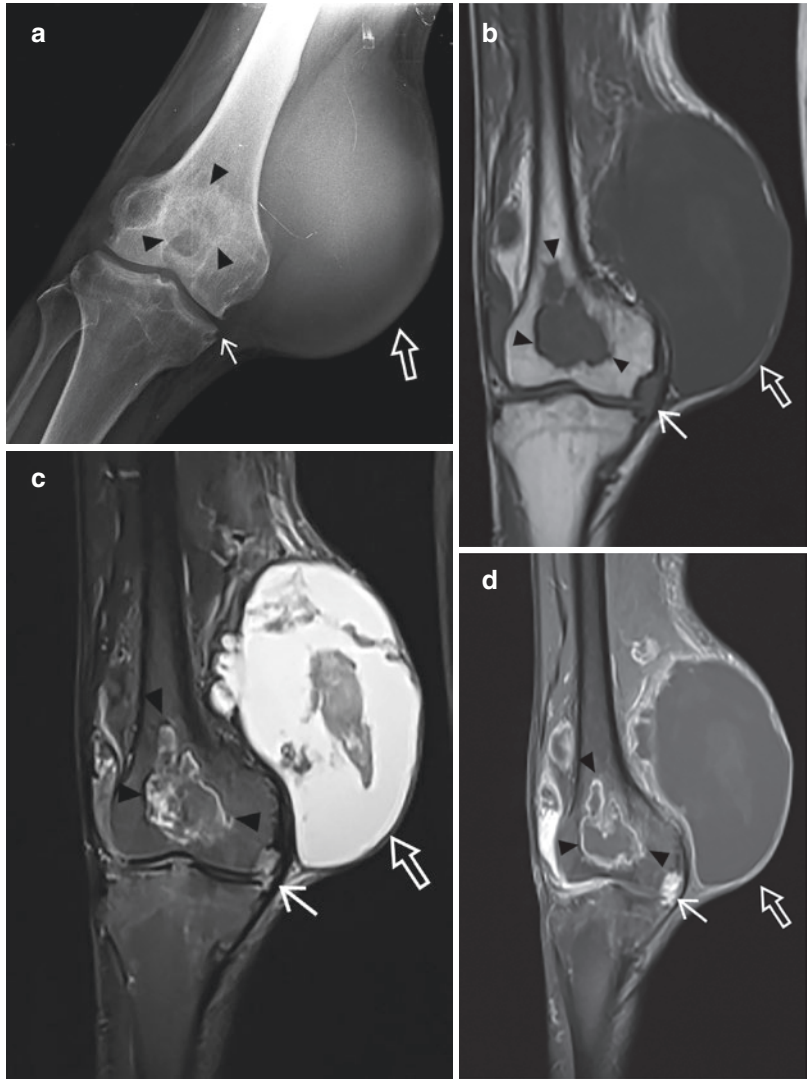
Fig. 19 Tuberculous osteomyelitis of the sternum in a 44-year-old woman who presented with a painless anterior chest wall mass. (a) Coronal CT image shows an osteolytic lesion at the right sternal border. (b) Coronal

and (c) axial contrast-enhanced fat-suppressed T1-weighted MR images of the sternum show an intraosseous abscess with anterior soft tissue extension (arrow)

Fig. 20 Tuberculous osteomyelitis of the chest wall in a 47-year-old woman with tricuspid valve replacement who presented with a painful left breast mass. Axial contrast-enhanced CT image shows a chest wall abscess at the left costochondral junction and mediastinal extension abutting the pericardium (arrow)



Fig. 21 Tuberculous osteomyelitis and arthritis, with an associated large soft tissue abscess in a 71-year-old man who had slow-growing thigh mass for the past 1 year. (a) Frontal radiograph of the right knee shows an osteolytic lesion in the femur with sclerotic borders (arrowheads), marginal bone erosion (arrow), and a large soft tissue mass (open arrow). Coronal (b) T1-weighted, (c) fat-suppressed T2-weighted, and (d) contrast-enhanced fat-suppressed T1-weighted MR images show osteomyelitis in the distal femur (arrowheads), synovial enhancement with bone erosion (arrows), and a large subcutaneous abscess (open arrows)



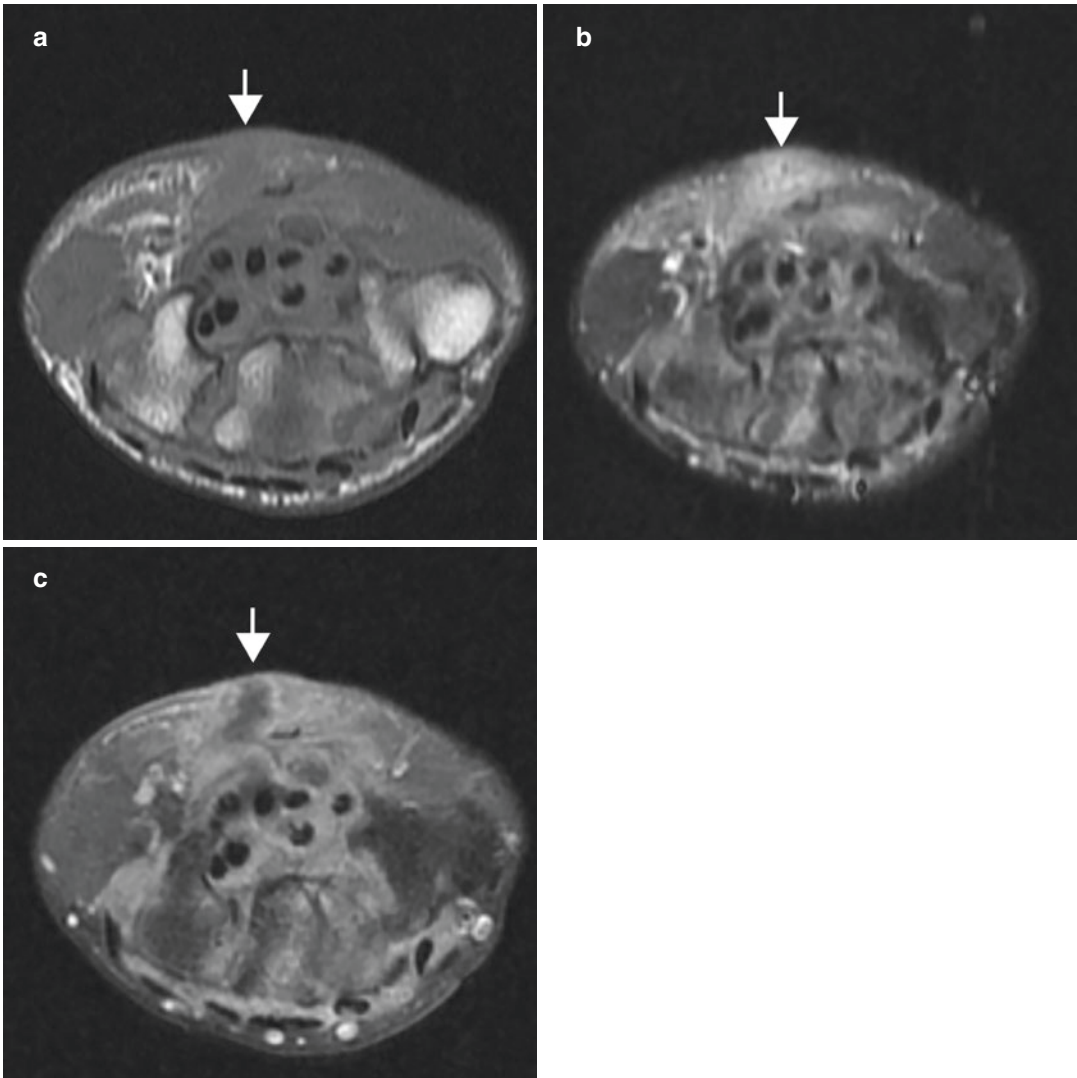


Fig. 22 Tuberculous arthritis and tenosynovitis with a sinus tract in a 41-year-old man who had wrist pain and a draining sinus for 6 months. Axial (a) T1-weighted, (b) STIR, and (c) contrast-enhanced fat-suppressed

T1-weighted MR images show bone marrow signal abnormality in the carpal bones, synovitis in the flexor tendon sheath, and a “tram-track” sinus tract (arrows)

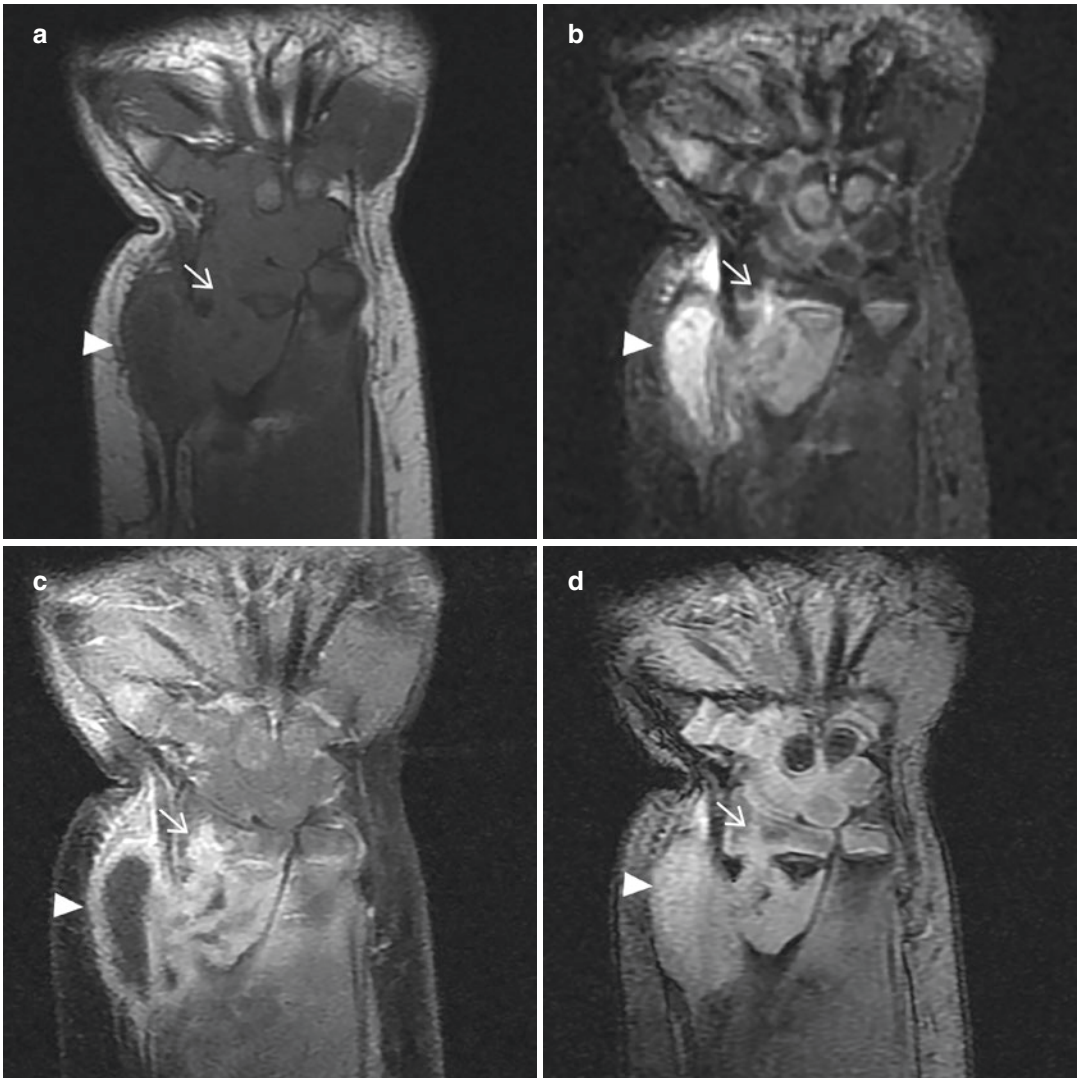


Fig. 23 Tuberculous osteomyelitis with transphyseal spread in a 1-year-old girl who had wrist pain and swelling for 1 month. Coronal (a) T1-weighted, (b) STIR, (c) contrast-enhanced fat-suppressed T1-weighted, and (d) 3D spoiled gradient-recalled (SPGR) MR images show

osteomyelitis in the metaphysis of the radius with transphyseal spread into the unossified epiphysis (arrows). Note extension to form an adjacent soft tissue abscess with the penumbra sign (arrowheads)

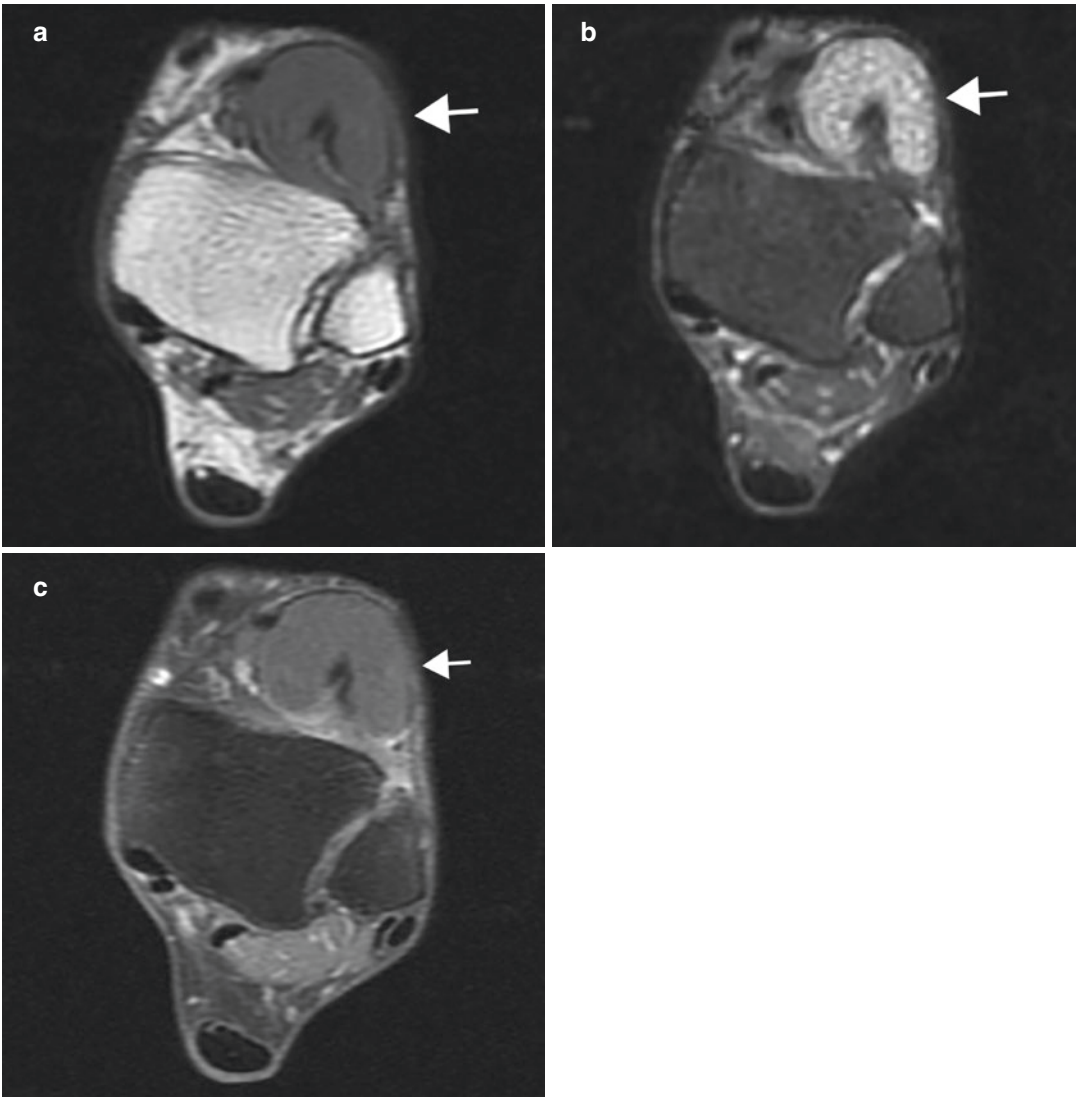


Fig. 24 Tuberculous tenosynovitis with rice bodies in a 70-year-old woman who had a soft tissue mass at the ankle for 1 year. Axial (a) T1-weighted, (b) T2-weighted, and (c) contrast-enhanced fat-suppressed T1-weighted

MR images show T2-hypointense rice bodies in the extensor digitorum tendon sheath (arrows). Note the rice bodies are imperceptible on the T1-weighted image and do not enhance

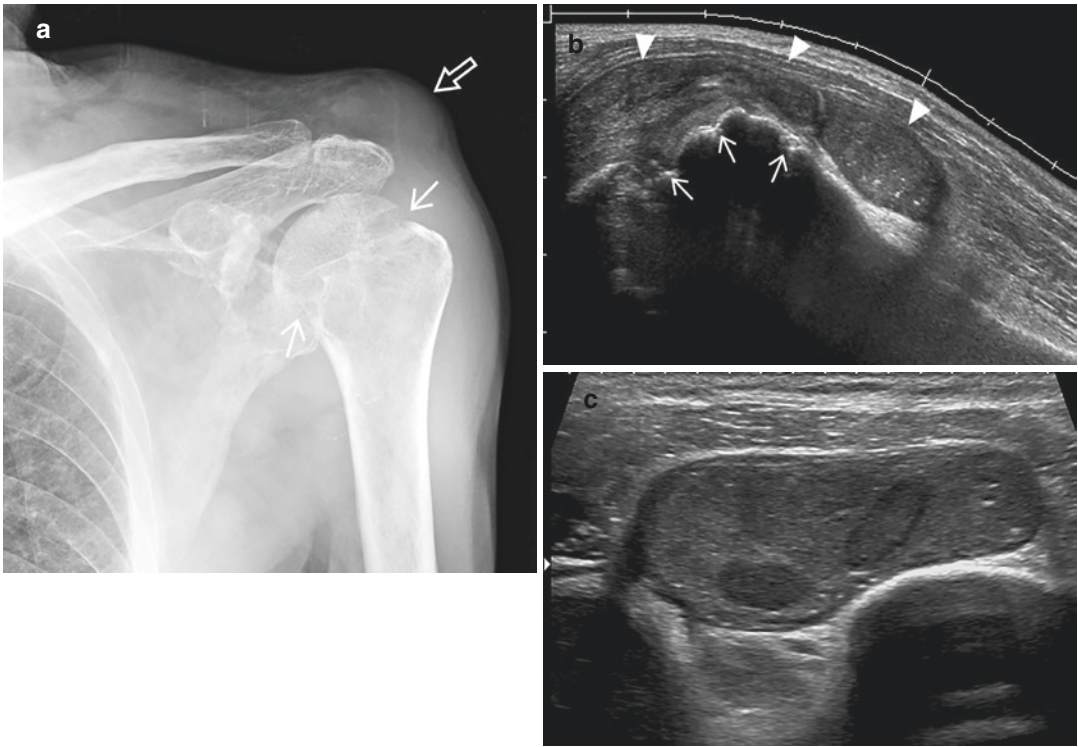


Fig. 25 Tuberculous arthritis of the left shoulder with subdeltoid bursitis in a 68-year-old man who had left shoulder pain for 10 months. (a) Frontal radiograph shows bone erosions (arrows) in the humeral head and soft tissue swelling (open arrow) superior to the shoulder joint. (b)

Longitudinal US image shows erosions in the humeral head (arrows) with echogenic effusion in the subdeltoid bursa (arrowheads). (c) Transverse US image of the shoulder shows rice bodies in the echogenic joint fluid within the subdeltoid bursa

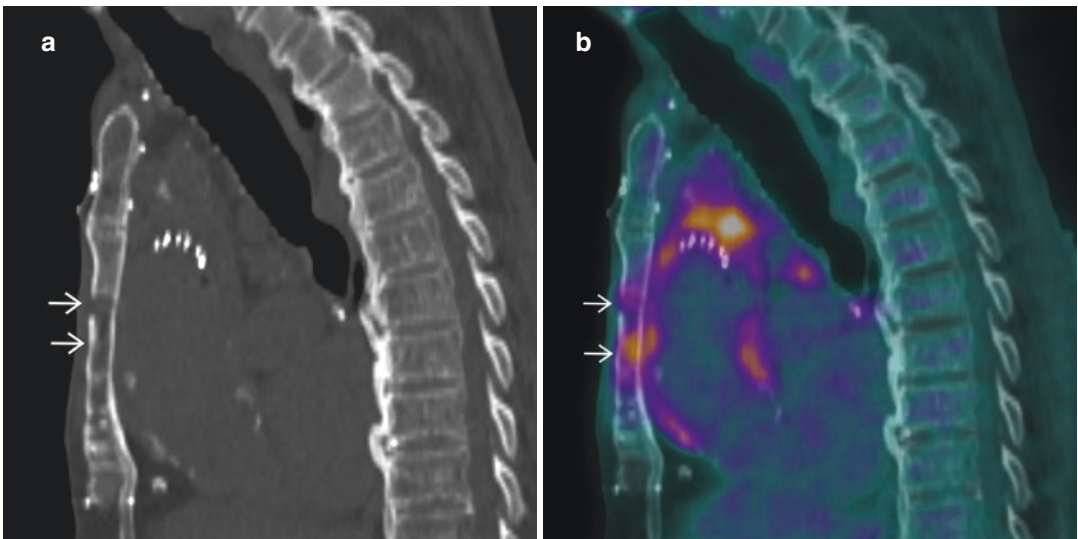


Fig. 26 ¹⁸F-FDG PET/CT of tuberculous osteomyelitis. 83-year-old man with thoracic aortic dissection who had prolonged fever after thoracic aortic stent-graft placement. Sagittal (a) CT and (b) PET/CT fusion images show an

intense metabolic-active destructive osteolytic lesion in the sternum (arrows). Biopsy revealed caseating granulomatous inflammation. (Courtesy of Dr. Tawika Kaewchur, Faculty of Medicine, Chiang Mai University, Thailand)

5 Imaging Differential Diagnosis

5.1 Tuberculous Osteomyelitis

Intraosseous abscesses cause well-defined osteolytic lesions mimicking tumor or tumor-like conditions such as simple bone cyst, aneurysmal bone cyst, chondroblastoma, or intraosseous tophi. Multifocal tuberculous osteomyelitis shares similar imaging features with eosinophilic granuloma, bone metastases, and multiple myeloma. The differential diagnosis of tuberculous dactylitis includes other conditions affecting short tubular bones such as vaso-occlusive insult of sickle cell disease, eosinophilic granuloma, and enchondroma (Ejindu et al. 2007; Ranjan et al. 2019). Tuberculous osteomyelitis of the femoral capital epiphysis in children can cause flattening and sclerotic changes, with an imaging appearance similar to Perthes disease (Agarwal 2020) (Fig. 5c). Presence of abscess formation, penumbra sign, and track-like transphyseal spread help in distinguishing abscesses from other conditions.

5.2 Tuberculous Arthritis

The clinical and radiological appearances of pyogenic arthritis and inflammatory arthritis share some similar features with tuberculous arthritis. Bone erosions, subchondral bone marrow edema, and inflammatory changes of the surrounding soft tissues due to pyogenic arthritis are more prominent than those of TB. The abscess walls in TB tend to be smooth and thin, while they are typically irregular and thick in pyogenic arthritis (Hong et al. 2001). Although rare, coexistent TB and pyogenic arthritis have been reported (Dojode et al. 2018). The main presumptive imaging signs of tuberculous arthritis are summarized in Table 1.

Rheumatoid arthritis typically presents as a symmetrical polyarticular disease. However, the

Table 1 Presumptive imaging signs of tuberculous arthritis

Subchondral bone	Osteopenia Mild bone sclerosis Large bone erosions containing sequestra Mild bone edema (on MRI)
Joint space	Slow and progressive narrowing Prominent synovial thickening Synovial calcifications Different age of synovitis (on MRI) Mild effusion with T2-hypointense signal (on MRI)
Soft tissues	Smooth wall abscess, with calcifications of the abscess wall

disease may initially manifest as a monoarticular involvement and persist in that stage for a long time. Both rheumatoid and tuberculous arthritis can cause juxta-articular osteoporosis and heterogeneous T2-hypointense synovitis. Synovitis related to rheumatoid arthritis tends to be uneven and thick, while tuberculous synovitis is smooth and thin. Large bone erosions and para-articular abscesses favor tuberculosis (Choi et al. 2009).

The destruction pattern of TB in the foot may mimic neuropathic joint disease. Tuberculous arthritis, particularly in the interconnected joints of midfoot, has potential for widespread destruction, similar to the pattern seen in neuropathic joint disease. In contrast to neuropathic joint, severe osteoporosis is the hallmark of tuberculous arthritis during the active stage (Dhillon and Nagi 2002). The presence of para-articular abscesses and draining sinus leads to the diagnosis of infectious arthritis (Zacharia et al. 2003) (Fig. 27).

On MRI, synovial chondromatosis manifests as intra-articular loose bodies with hypointense signal on T2-weighted images, similar to that of rice bodies. However, on T1-weighted images, the signal intensity of synovial chondromatosis loose bodies is hyperintense, while that of rice bodies of TB are almost imperceptible (Chen et al. 2002) (Fig. 28).



Fig. 27 Tuberculous arthritis in a 33-year-old woman who had left foot pain and a draining sinus in the dorsal foot for 1 month. **(a)** Frontal radiograph shows narrowing of the joint spaces of the midfoot and Lisfranc joint subluxation (open arrow), resembling a neuropathic joint. Coronal **(b)** fat-suppressed T2-weighted and **(c)** contrast-

enhanced fat-suppressed T1-weighted MR images show extensive bone marrow edema and enhancement of the midfoot bones. Note the inflammation of the dorsal subcutaneous soft tissues (arrows) corresponding to the location of the sinus tract

5.3 Tuberculous Soft Tissue Infection

Tuberculous myositis and bursitis can present as a slow-growing mass that clinically simulates a tumor (Batra et al. 2007). Infection tends to spread along the low resistant space under the fascia (Soler et al. 2001). CT, MRI, and US imaging allow detection of the abscess and evaluation of the extent of disease. The calcifi-

cation of granulomatous tissue at the wall of abscesses is characteristic of TB, but can also be a feature of other chronic bacterial infections (Coppola et al. 1987; Pattamapaspong and Muttarak 2011). Tuberculous abscesses of the anterior chest wall can be clinically confused with breast masses (Chung et al. 1996; Arslan et al. 1999; Jain et al. 2009; Teo et al. 2009) (Fig. 20). CT and MRI help confirm the precise location of the disease.

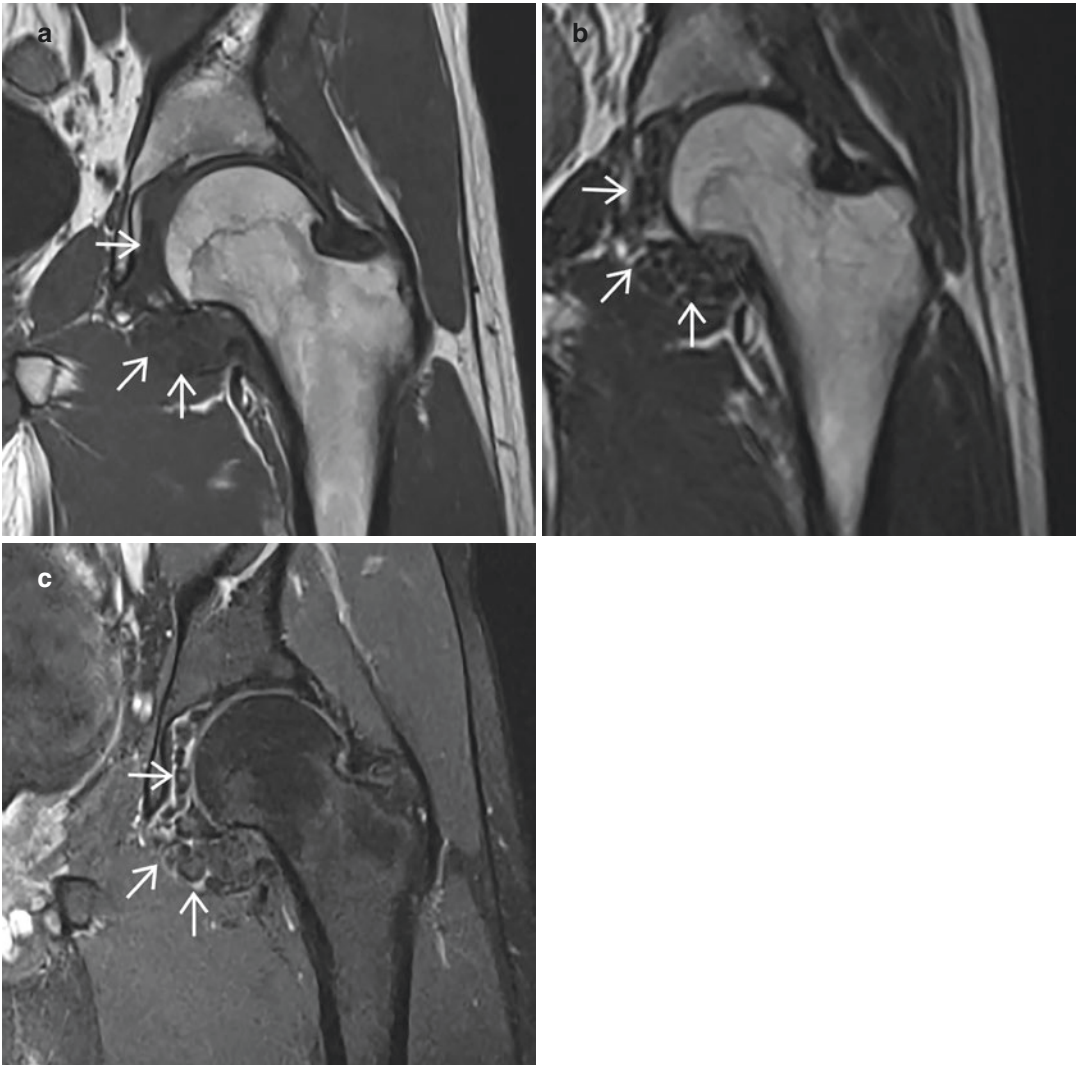


Fig. 28 Synovial chondromatosis. Coronal (a) T1-weighted, (b) T2-weighted, and (c) contrast-enhanced fat-suppressed T1-weighted MR images of the left hip

show osteochondral bodies which show faintly T1-hyperintense signal, T2-hypointense signal and do not enhance (arrows)

6 Diagnosis Confirmation

The definite diagnosis of musculoskeletal TB requires positive culture or smear microscopy from pus or infected tissue. However, smear microscopy has a low sensitivity (less than 40%), causing difficulty in diagnosis (Natarajan et al. 2020). Culture may yield 80% sensitivity but takes 6–8 weeks, resulting in a delay of treatment and potential further structural damages (Gardam and Lim 2005). Molecular meth-

ods examining for the presence of *M. tuberculosis*-specific DNA in biopsy and cytology specimens provide timely reliable diagnostic results and early identification of drug-resistant strains (Ghanekar et al. 2019; Natarajan et al. 2020). The histopathological findings of granulomatous and necrotizing inflammatory reaction, although non-specific, help suggest the diagnosis of TB. Infected specimens should be taken from the depth of the infected site to avoid contamination by other

organisms at the sinus tract. In endemic areas or in patients with a risk of exposure to TB, diagnosis that is based on the combination of clinical, imaging, and histopathological findings is practically acceptable (Ghanekar et al. 2019).

7 Treatment

Musculoskeletal TB is typically treated using anti-TB drugs. The optimal treatment duration remains debatable but a 9–12 month course is recommended (Nahid et al. 2016). Surgical intervention aims to facilitate healing, prevent the spread of the infection, and maintain function. If performed, debridement needs to include sinus tracts which may not be possible by the standard incision; thus imaging plays a role in surgical planning (Dhillon et al. 2017). Arthrodesis or arthroplasty may be necessary in order to relieve pain and maintain function. Surgery can provide successful outcome when combined with adequate anti-TB drug treatment (Dhillon et al. 2017; Parsa et al. 2018).

The response to treatment is judged by clinical and radiological improvement. Clinically, fever, night sweats, weight loss, and draining sinuses should resolve. Radiological signs of healing include resolution of abscesses and bone marrow edema, with gradual remineralization of affected bones. No improvement or deterioration of the disease after five months of treatment should raise the concern of treatment failure. Follow-up for at least 2 years after completing the course of treatment is recommended for monitoring of possible disease relapse (World Health Organization and Ministry of Health and Family Welfare, Government of India 2016).

8 Conclusion

Extraplural musculoskeletal TB has various clinical manifestations and imaging findings, depending on whether the affected sites are the bone, joint, or soft tissues. Imaging studies are valuable tools in lesion detection and achieving an accurate diagnosis, bearing in mind that TB can mimic

a number of other musculoskeletal diseases. Although non-specific, certain patterns of structural destruction accompanied by abscesses with minimal inflammatory reaction, soft tissue calcification and sinus tracts are suggestive of TB. When combined with the appropriate clinical context, these characteristic imaging features lead to timely diagnosis and appropriate treatment.

References

- Agarwal A (2020) Paediatric osteoarticular tuberculosis: a review. *J Clin Orthop Trauma* 11:202–207
- Akeson WH, Chu CR, Bugbee W (2002) Articular cartilage: morphology, physiology, and function. In: Resnick D (ed) *Diagnosis of bone and joint disorders*, 4th edn. W.B. Saunders, Philadelphia, pp 793–815
- Ankrah AO, Van der Werf TS, De Vries EF et al (2016) PET/CT imaging of *Mycobacterium tuberculosis* infection. *Clin Transl Imaging* 4:131–144
- Arora VK, Chopra KK (2019) Geriatric TB: Needs focussed attention under RNTCP. *Indian J Tuberc* 66:516–519
- Arslan A, Ciftci E, Yildiz F et al (1999) Multifocal bone tuberculosis presenting as a breast mass: CT and MRI findings. *Eur Radiol* 9:1117–1119
- Batra S, Ab Naell M, Barwick C et al (2007) Tuberculous pyomyositis of the thigh masquerading as malignancy with concomitant tuberculous flexor tenosynovitis and dactylitis of the hand. *Singapore Med J* 48:1042–1046
- Bergeron EJ, Meguid RA, Mitchell JD (2017) Chronic infections of the chest wall. *Thorac Surg Clin* 27:87–97
- Bryan WJ, Doherty JH Jr, Sculco TP (1982) Tuberculosis in a rheumatoid patient. A case report. *Clin Orthop Relat Res* 171:206–208
- Carrega G, Bartolacci V, Burastero G, Finocchio GC, Ronca A, Riccio G (2013) Prosthetic joint infections due to *Mycobacterium tuberculosis*: a report of 5 cases. *Int J Surg Case Rep* 4:178–181
- Chen A, Wong LY, Sheu CY et al (2002) Distinguishing multiple rice body formation in chronic subacromial-subdeltoid bursitis from synovial chondromatosis. *Skeletal Radiol* 31:119–121
- Choi JA, Koh SH, Hong SH et al (2009) Rheumatoid arthritis and tuberculous arthritis: differentiating MRI features. *AJR Am J Roentgenol* 193:1347–1353
- Chung SY, Yang I, Bae SH et al (1996) Tuberculous abscess in retromammary region: CT findings. *J Comput Assist Tomogr* 20:766–769
- Coppola J, Muller NL, Connell DG (1987) Computed tomography of musculoskeletal tuberculosis. *Can Assoc Radiol J* 38:199–203
- De Backer AI, Morteel KJ, Vanhoenacker FM et al (2006) Imaging of extrapural musculoskeletal tuberculosis. *Eur Radiol* 57:119–130

- De Vuyst D, Vanhoenacker F, Gielen J et al (2003) Imaging features of musculoskeletal tuberculosis. *Eur Radiol* 13:1809–1819
- Dhillon MS, Agashe V, Patil SD (2017) Role of surgery in management of osteo-articular tuberculosis of the foot and ankle. *Open Orthop J* 11:633–650
- Dhillon MS, Nagi ON (2002) Tuberculosis of the foot and ankle. *Clin Orthop Relat Res* 398:107–113
- Dojode CMR, Joseph G, Shah NN (2018) A deceptive presentation of tuberculosis hip as staphylococcal infection, its successful management and literature review. *BMJ Case Rep* 2018:bcr-2018-224558. <https://doi.org/10.1136/bcr-2018-224558>
- Ejindu VC, Hine AL, Mashayekhi M et al (2007) Musculoskeletal manifestations of sickle cell disease. *Radiographics* 27:1005–1021
- Forse CL, Mucha BL, Santos MLZ, Ongcapin EH (2012) Rice body formation without rheumatic disease or tuberculosis infection: a case report and literature review. *Clin Rheumatol* 31:1753–1756
- Gardam M, Lim S (2005) Mycobacterial osteomyelitis and arthritis. *Infect Dis Clin North Am* 19:819–830
- Ghanekar C, Patel D, Abhyankar M et al (2019) Role of line probe assay in detection of extra-pulmonary tuberculosis: experience from a tertiary care hospital in western Maharashtra. *Indian J Tuberc* 66:325–330
- Gopal K, Raj A, Rajesh MR et al (2007) Sternal tuberculosis after sternotomy for coronary artery bypass surgery: a case report and review of the literature. *J Thorac Cardiovasc Surg* 133:1365–1366
- Grey AC, Davies AM, Mangham DC et al (1998) The ‘penumbra sign’ on T1-weighted MR imaging in sub-acute osteomyelitis: frequency, cause and significance. *Clin Radiol* 53:587–592
- Griffith JF, Peh WCG, Evans NS, Smallman LA, Wong RW, Thomas AM (1996) Multiple rice body formation in chronic subacromial/subdeltoid bursitis: MR appearances. *Clin Radiol* 51:511–514
- Harwin SF, Banerjee S, Issa K et al (2013) Tubercular prosthetic knee joint infection. *Orthopedics* 36:e1464–e1469
- Hassanpour SE, Gousheh J (2006) Mycobacterium tuberculosis-induced carpal tunnel syndrome: management and follow-up evaluation. *J Hand Surg Am* 31:575–579
- Hodkinson B, Musenge E, Tikly M (2009) Osteoarticular tuberculosis in patients with systemic lupus erythematosus. *QJM* 102:321–328
- Hong SH, Kim SM, Ahn JM et al (2001) Tuberculous versus pyogenic arthritis: MR imaging evaluation. *Radiology* 218:848–853
- Hortas C, Ferreira JL, Galdo B et al (1988) Tuberculous arthritis of peripheral joints in patients with previous inflammatory rheumatic disease. *Br J Rheumatol* 27:65–67
- Hsu CY, Lu HC, Shih TT (2004) Tuberculous infection of the wrist: MRI features. *AJR Am J Roentgenol* 183:623–628
- Hugate R Jr, Pellegrini VD Jr (2002) Reactivation of ancient tuberculous arthritis of the hip following total hip arthroplasty: a case report. *J Bone Joint Surg Am* 84:101–105
- Jain S, Shrivastava A, Chandra D (2009) Breast lump, a rare presentation of costochondral junction tuberculosis: a case report. *Cases J* 2:7039
- Jaovisidha S, Chen C, Ryu KN et al (1996) Tuberculous tenosynovitis and bursitis: imaging findings in 21 cases. *Radiology* 201:507–513
- Khater FJ, Samnani IQ, Mehta JB, Moorman JP, Myers JW (2007) Prosthetic joint infection by *Mycobacterium tuberculosis*: an unusual case report with literature review. *South Med J* 100:66–69
- Kumar S, Agarwal A, Arora A (2006) Skeletal tuberculosis following fracture fixation. A report of five cases. *J Bone Joint Surg Am* 88:1101–1106
- Lin JN, Lai CH, Chen YH et al (2009) Risk factors for extra-pulmonary tuberculosis compared to pulmonary tuberculosis. *Int J Tuberc Lung Dis* 13:620–625
- McGuinness B, Wilson N, Doyle AJ (2007) The ‘penumbra sign’ on T1-weighted MRI for differentiating musculoskeletal infection from tumour. *Skeletal Radiol* 36:417–421
- Morris BS, Maheshwari M, Chalwa A (2004) Chest wall tuberculosis: a review of CT appearances. *Br J Radiol* 77:449–457
- Nag HL, Neogi DS, Nataraj AR et al (2009) Tubercular infection after arthroscopic anterior cruciate ligament reconstruction. *Arthroscopy* 25:131–136
- Nahid P, Dorman SE, Alipanah N et al (2016) Official American Thoracic Society/Centers for Disease Control and Prevention/Infectious Diseases Society of America Clinical Practice Guidelines: Treatment of drug-susceptible tuberculosis. *Clin Infect Dis* 63:e147–e195
- Naidoo J, Mahomed N, Moodley H (2017) A systemic review of tuberculosis with HIV coinfection in children. *Pediatr Radiol* 47:1269–1276
- Natarajan A, Beena PM, Devnikar AV et al (2020) A systemic review on tuberculosis. *Indian J Tuberc* 67:295–311
- Palestro CJ, Love C, Miller TT (2006) Infection and musculoskeletal conditions: imaging of musculoskeletal infections. *Best Pract Res Clin Rheumatol* 20:1197–1218
- Parsa A, Mirzaie M, Ebrahimzadeh MH et al (2018) Hip surgery in quiescent or active tubercular hip arthritis: is reactivation risk really a matter. *Arch Bone Jt Surg* 6:169–175
- Pattamapaspong N, Muttarak M (2011) Musculoskeletal melioidosis. *Semin Musculoskelet Radiol* 15:480–488
- Perez-Velez CM, Marais BJ (2012) Tuberculosis in children. *N Engl J Med* 367:348–361
- Phemister DB, Hatcher CH (1933) Correlation of pathological and roentgenological findings in the diagnosis of tuberculous arthritis. *AJR Am J Roentgenol* 29:736–752
- Pigrau-Serrallach C, Rodríguez-Pardo D (2013) Bone and joint tuberculosis. *Eur Spine J* 22(Suppl. 4):556–566
- Popert J (1985) Rice-bodies, synovial debris, and joint lavage. *Br J Rheumatol* 24:1–2

- Prasad A, Manchanda S, Sachdev N et al (2012) Imaging features of pediatric musculoskeletal tuberculosis. *Pediatr Radiol* 42:1235–1249
- Ranjan R, Goel L, Sud A et al (2019) Bilateral tubercular dactylitis: unusual presentation of an usual disease. *Indian J Tuberc* 66:346–352
- Ranson M (2009) Imaging of pediatric musculoskeletal infection. *Semin Musculoskelet Radiol* 13:277–299
- Resnick D (2002a) Osteomyelitis, septic arthritis, and soft tissue infection: mechanisms and situations. In: Resnick D (ed) *Diagnosis of bone and joint disorders*, 4th edn. W.B. Saunders, Philadelphia, pp 2377–2480
- Resnick D (2002b) Osteomyelitis, septic arthritis, and soft tissue infection: organisms. In: Resnick D (ed) *Diagnosis of bone and joint disorders*, 4th edn. W.B. Saunders, Philadelphia, pp 2510–2624
- Sawlani V, Chandra T, Mishra RN et al (2003) MRI features of tuberculosis of peripheral joints. *Clin Radiol* 58:755–762
- Sharma SV, Varma BP, Khanna S (1978) Dystrophic calcification in tubercular lesions of bursae. *Acta Orthop Scand* 49:445–447
- Shikhare SN, Singh DR, Shimpi TR, Peh WCG (2011) Tuberculous osteomyelitis and spondylodiscitis. *Semin Musculoskelet Radiol* 15:446–458
- Soler R, Rodriguez E, Remuinan C et al (2001) MRI of musculoskeletal extrapural tuberculosis. *J Comput Assist Tomogr* 25:177–183
- Suarez I, Maria Funger S, Jung N et al (2019) Severe disseminated tuberculosis in HIV-negative refugees. *Lancet Infect Dis* 19:e352–e359
- Subramaniam R, Tan JWL, Chau CYP, Lee KT (2012) Subacromial bursitis with giant rice bodies as initial presentation of rheumatoid arthritis. *J Clin Rheumatol* 18:352–355
- Suh JS, Lee JD, Cho JH (1996) MR imaging of tuberculous arthritis: clinical and experimental studies. *J Magn Reson Imaging* 6:185–189
- Teo TH, Ho GH, Chaturverdi A et al (2009) Tuberculosis of the chest wall: unusual presentation as a breast lump. *Singapore Med J* 50:e97–e99
- Tiwari A, Sud A, Mehta S (2007) Multifocal skeletal tuberculosis presenting as multiple bone cysts. *Ann Acad Med Singapore* 36:1038–1039
- Wang MN, Chen WM, Lee KS (1999) Tuberculous osteomyelitis in young children. *J Pediatr Orthop* 19:151–155
- World Health Organization (2021) *Global tuberculosis report 2021*. World Health Organization, Geneva. Available at: <https://www.who.int/teams/global-tuberculosis-programme/tb-reports/global-tuberculosis-report-2021>
- World Health Organization and Ministry of Health and Family Welfare, Government of India (2016) *Index—TB Guidelines*. In: *Guidelines on extrapulmonary tuberculosis for India*. World Health Organization, Geneva. Available at: <https://tbcindia.gov.in/showfile.php?lid=3245>. Accessed 17 May 2021
- Zacharia TT, Shah JR, Patkar D et al (2003) MRI in ankle tuberculosis: review of 14 cases. *Australas Radiol* 47:11–16